JPP Journal of Pharmacy and Pharmacology
ROYAL PHARMACEUTICAL SOCIETY

JPP Journal of Pharmacy and Pharmacology

Research Paper

JPP 2011, 63: 352–361

Received July 23, 2010
Accepted October 22, 2010
DOI
10.1111/j.2042-7158.2010.01226.x
ISSN 0022-3573

Supersaturated dissolution data and their interpretation: the TPGS–carbamazepine model case

Georgia Charkoftaki, Aristides Dokoumetzidis, Georgia Valsami and Panos Macheras

Laboratory of Biopharmaceutics-Pharmacokinetics, Faculty of Pharmacy, University of Athens, Panepistimiopolis 157 71, Athens, Greece

Abstract

Objectives This study was undertaken to investigate the effect of D-alpha-tocopheryl polyethylene glycol 1000 succinate (vitamin E TPGS) on the dissolution of carbamazepine (CBZ) commercial tablets (Tegretol®) as a function of temperature and to modify the reaction-limited model of dissolution for the description of classical supersaturated dissolution data.

Methods Solubility studies were performed using various concentrations of (i) TPGS and (ii) silicon dioxide and microcrystalline cellulose, which are excipients of Tegretol® at 10, 25 and 37°C. Dissolution studies were carried out using Tegretol® tablets, 200 mg/tab.

Key findings The solubility of CBZ in the presence of TPGS was found to increase in a concentration-dependent manner at all temperatures studied. Classical supersaturated dissolution curves with concentration maxima higher than the corresponding solubility values in the presence of TPGS were observed only at 10°C. The model developed was based on a time-dependant expression for the forward microconstant of the CBZ-TPGS reaction at the solid–liquid interface and it was fitted successfully to the dissolution data of CBZ in the presence of TPGS at 10°C.

Conclusions Vitamin E TPGS increased the solubility of CBZ at all temperatures studied. The modification of the reaction-limited model of dissolution allowed us to describe classical supersaturated dissolution curves.

Keywords carbamazepine; dissolution; solubility; supersaturation; vitamin E TPGS

Introduction

Drug dissolution is a critical process for almost all orally administered drug products. It sets quality control standards for drug delivery, specifications for research when designing dosage forms and since 1980 there has been an emphasis on dissolution as a prognostic tool of oral drug absorption. The paddle apparatus is the most commonly used, and numerous dissolution tests have been performed in order to characterize the release of drug from formulation. The majority of dissolution profiles are of monotonic nature, with an initial increase of drug dissolution that reaches a plateau value at a certain time point. This value indicates either a saturation level or 100% dissolution (release).

As more and more poorly water-soluble compounds are being produced, leading to problematic biopharmaceutical properties, many approaches have been developed to improve the solubility and dissolution rate of these substances. Modifications to the drug substance or to the physicochemical properties of the formulation have been adopted to achieve better drug solubility.[1] Cogrinding or comelting a compound with surfactants, such as sodium lauryl sulphate, hydroxypropyl methyl cellulose or polyvinylpyrolidone, is also very popular. These techniques often result in increased solubility for the poorly soluble compounds and in unusual supersaturated, non-monotonic dissolution profiles.[2–8] In-vitro solubility studies demonstrate solubility values after the addition of surfactants or polymers that are many times higher than the aqueous solubility of the compound alone.[9–12]

There are studies showing the creation of supersaturated solutions in aspirated human intestinal fluids.[13–16] Studies dealing with supersaturated dissolution data for poorly water-soluble drugs are divided into two categories, which are discussed below.

In the first set of the studies, the preparation of a high-energy metastable form of the drug in an amorphous or semicrystalline state is described.[17–19] Usually, the solubility of the

Correspondence: Panos Macheras, Faculty of Pharmacy, Laboratory of Biopharmaceutics-Pharmacokinetics, University of Athens, Panepistimiopolis 157 71, Athens, Greece.
E-mail: macheras@pharm.uoa.gr

amorphous polymorphs is much higher than that of its crystalline form.[18] This results in an increased dissolution rate and an enhancement of bioavailabity.[20,21] However, it is not uncommon to observe a progressive diminution of drug concentration during the dissolution process due to the kinetic instability of the high-energy amorphous drug.[21,22] This type of study of the enhanced-solubility dissolution rate is routinely explained via the increased solubility of the drug C_s in accord with the Noyes–Whitney equation:

$$\frac{dC}{dt} = \frac{DA}{h}(C_s - C) \quad (1)$$

where D is the diffusivity, A is the specific area of the particles, h is the diffusion layer path length in the boundary layer about the particle, and C is the concentration of drug in solution at time t.

In the second set of studies, the dissolution of poorly soluble drugs is studied in the presence of various additives, e.g. surfactant agents, polymers and food constituents.[21–24] A very high initial dissolution rate is usually observed, which leads to concentration values higher than the solubility level. When these higher-than-saturation solubility values are maintained and are justified by independent solubility experiments in the presence of additives, the high rate of dissolution can be explained on the basis of Equation 1. However, in several studies the supersaturated levels subsequently relax towards the saturation solubility.[21–26] This type of non-monotonic dissolution curve cannot be explained using the classical diffusion layer model (Equation 1).

A small number of modelling approaches have been proposed so far for the analysis of supersaturated data.[27–31] However, only one of them relies on the prevailing diffusion layer model for the description of the initial portion of the dissolution curve followed by a precipitation step.[30]

Most of the dissolution studies dealing with supersaturated phenomena are usually carried out with either the pure drug or the pure drug in the presence of additives. For example, the dissolution of pure carbamazepine (CBZ) exhibits supersaturation behaviour due to the transition between its polymorphs, and it has been the subject of several studies.[28,32,33] However, this type of study does not deal with the potential effect of excipients in the solubility–dissolution drug profile. Hence, the main purpose of the present study was to elucidate the complexity of CBZ dissolution in the presence of D-alpha-tocopheryl polyethylene glycol 1000 succinate (vitamin E TPGS) using commercially available CBZ tablets. TPGS is a non-ionic surfactant (hydrophilic–lipophilic balance (HLB) ~13), which has been found to enhance the solubility and absorption of poorly water-soluble drugs.[34,35] Solubility studies of pure CBZ were therefore carried out in the presence of TPGS and excipients, with various TPGS concentrations and temperatures. In addition, dissolution studies of the commercial tablets of CBZ were carried out, in the same TPGS concentrations and temperatures, as in solubility studies.

In order to investigate the potential effect of TPGS and excipients on CBZ's solubility–dissolution behaviour as a function of time, the dissolution experiments were performed for a much longer time (i.e. 48 h) than usual. Finally, another purpose of the present study was to develop a new model for interpreting classical supersaturated data.

Materials and Methods

Materials

CBZ powder was obtained from Novartis (ID: 002183.4, Novartis, Hellas) and Tegretol® tablets 200 mg/tab (Lot #E97L2287) were also obtained from Novartis. vitamin E TPGS (national formulary (NF)), was kindly provided by Eastman Chemical Company, Anglesey, UK (Batch #68104000, UK). Microcrystalline cellulose NF (Avicel®) was obtained from FMC BioPolymer (Lot #60706C, Ireland). Colloidal silicon dioxide USP/NF (Aerosil® 200 Pharma) was from Degussa (Bulk #3.8014.00001.00, Germany). Acetonitrile and methanol of HPLC grade were from E. Merck (Darmstad, Germany). Water purified with Labconco Water PRO PS system (Kansas City, MO). All other chemicals were of analytical grade.

Solubility studies of carbamazepine

Solubility and dissolution studies of CBZ were performed in the presence of vitamin E TPGS, a surfactant with amphiphilic properties (HLB ~13), which is a water-soluble derivative of natural source vitamin E.

More specifically, solubility studies of CBZ were performed at various concentrations of vitamin E TPGS (0, 0.5, 2.0 and 4.0 mM), at 10, 25 and 37°C, under a constant shaking rate of 50 rpm, for 24 h. These studies were conducted prior to the dissolution experiments, using the same aqueous media as in the dissolution studies. In addition, solubility studies in the absence and presence of silicon dioxide and microcrystalline cellulose, which are excipients of the Tegretol® formulation, were also performed at the same conditions as described above. The amount of colloidal silicon dioxide added to the aqueous medium was 0.35 and 0.70 mg, while that of microcrystalline cellulose was 40 and 70 mg; these values correspond to those usually encountered in the actual excipient ranges of commercial tablets. Initial solubility studies were performed in order to determine the time that equilibrium solubility was achieved. The results indicated that the equilibrium is achieved at 24 h. The experimental procedure in all cases was as follows: 5 mg of CBZ powder was added to a 25 ml flask containing 15 ml of the appropriate aqueous medium. The flasks were placed in a thermostated water bath at 10, 25 and 37°C under constant shaking rate of 50 rpm for 24 h. The sample was filtrated through regenerated cellulose filter (17 mm, 0.45 μm Titan®, Wilmington, DE). The first 0.2 ml was discarded in order to saturate the filter with the drug.

Dissolution studies of carbamazepine

Dissolution studies were carried out using a commercially available formulation of CBZ (Tegretol®), 200 mg/tab. All dissolution tests were performed using the USP II apparatus (paddle method) and were conducted in triplicate at 10, 25 and 37°C (±0.5°C). Dissolution experiments were performed using as dissolution media, 500 ml of aqueous TPGS solution in various concentrations: 0, 0.5, 2 and 4 mM. TPGS is an

excipient that is not present in the commercial tablet of CBZ (Tegretol®). The rotation speed was set at 50 rpm. A 5 ml sample was withdrawn at 5, 10, 15, 20, 25, 30, 45, 60, 90, 120, 150 min, 6, 24 and 48 h. Each sample was replaced with fresh dissolution medium. A syringe with a stainless-steel cannula was used to draw up the test solution. The sample was filtrated through a regenerated cellulose syringe filter (17 mm, 0.45 μm Titan®, Wilmington, DE). The first 0.2 ml was discarded in order to saturate the filter with the drug.

Drug analysis

The chromatography system used was an HPLC from GBC Scientific Equipment Pty Ltd (Melbourne, Australia) consisting of a LC 1120 HPLC pump solvent delivery system, an LC 1210 UV/Vis Detector and Clarity® chromatographic software. An isocratic HPLC method with detection at 285 nm was applied for CBZ assay. The mobile phase consisted of acetonitrile–H_2O at a volume ratio of 65 : 35 v/v. The flow rate was 1 ml/min, and the column type was Bischoff® ODS2 RP-C18 (250 mm × 4.6 mm, 5 μm particle size). The elution time for CBZ was approximately 3.6 min. Injection volume was 50 μl.

The reaction-limited model of dissolution

A reaction-limited model of dissolution was postulated during the initial physicochemical era of dissolution work, long time ago before the interest for drug dissolution arose. As early as 1933 Miyamoto explained the classical Noyes–Whitney relationship using Boltzman's thermodynamic principles.[36] Because of the lack of a solid mathematical description, the use of the reaction-limited model of dissolution was confined to the rotating disk apparatus, whereas hydrodynamic conditions are fully controlled. In fact, the contribution of the two concurrent mechanisms, namely, the interfacial transport and the diffusion of species through the stagnant layer of the particle, to the overall dissolution is dependent on the hydrodynamic conditions.[37] One of the two dissolution mechanisms becomes predominant at either of the two extremes (low and high) of agitation.[37]

Recently, a reaction-limited model was developed and found to be capable of a description of dissolution data of official dissolution tests.[29] The model relies on the bidirectional chemical reaction of the solid species s with n free solvent molecules w, yielding the dissolved species of the drug complex with solvent c:

$$s + n\,w \underset{k_{-1}}{\overset{k_1}{\rightleftharpoons}} c \qquad (2)$$

where k_1 and k_{-1} are the forwards and backwards microconstants. The major characteristic of this model is that the rate of dissolution is not governed by the saturation solubility. The saturation solubility of the drug in the dissolution medium, C_s, is the result of the chemical equilibrium of Equation 2 and corresponds to the concentration at steady state, C_{ss}, when the drug dose, M_0, is in excess:

$$C_{ss} = \frac{k_1^*}{k_1^* + k_{-1}} \frac{M_0}{V} \qquad (3)$$

where V is the volume of the dissolution medium and k_1^* is a composite rate constant related to k_1.[27]

Statistical analysis

The effect of vitamin E TPGS on CBZ solubility and maximum dissolution concentration, at the three different temperatures, was examined statistically by paired t-test, since the normality test was passed in all cases. A significance level of $P < 0.05$ denoted significance in all cases. All solubility and dissolution studies were performed in triplicate. Statistical analysis was performed using SigmaStat 2.03 statistical software (SPSS Inc.).

Fittings of the model of Equations 4 and 6 were performed using the routine 'lsqnonlin' in MATLAB, while the standard errors of the parameter estimates were calculated using the Fisher Information Matrix, also in MATLAB, and were expressed as coefficients of variation (CV).

Results

CBZ's dissolution profiles in water, in the presence and absence of TPGS, at 10, 25 and 37°C, are shown in Figures 1–3. The inserts in these figures show the dissolution profiles up to 2.5 h. Estimates for CBZ saturation solubility in the same media and at the same temperatures as the dissolution experiments, are listed in Table 1. For comparative purposes, the maximum concentration values observed in the dissolution experiments are also listed in Table 1. Figure 4 provides a pictorial view of the relationship between the saturation solubility and the maximum concentration values recorded in the dissolution experiments in the absence and presence of TPGS at the three temperatures studied. The results from the solubility studies that were performed in the presence of the two excipients, either microcrystalline cellulose or silicon dioxide, are listed in Table 2.

Discussion

The description of the dissolution behaviour of CBZ tablets in the presence of a surfactant, at various temperatures, is very complex. It is not only CBZ's polymorphism[36] that makes this description complicated (Figures 1–3): the time- and temperature-dependent effects of the excipients and the surfactant (TPGS), which supplement micelle-mediated dissolution, result in complicated dissolution profiles.

CBZ has four known anhydrous polymorphic forms and a dihydrate.[38] The commercial form of CBZ is form III (P-monoclinic), which converts to a less soluble, dihydrate form.[32,39] Recently, the transformations of form III were investigated.[40] This study revealed CBZ's conversion stages from the anhydrous to the dihydrate form.[40] Initially, there is a pre-transformation stage, which is followed by a transformation stage and a steep diminution resulting in a steady-state stage of CBZ, in which both forms exist (i.e. it is not 100% converted to hydrate form).[33,40] The duration of the transformation stage is highly affected by surfactants: in their absence, the steady state is reached after 13 h, while in the presence of surfactants this time is significantly reduced (7.4 h). This conclusion is in agreement with the pattern of the dissolution profiles observed in our study at the same

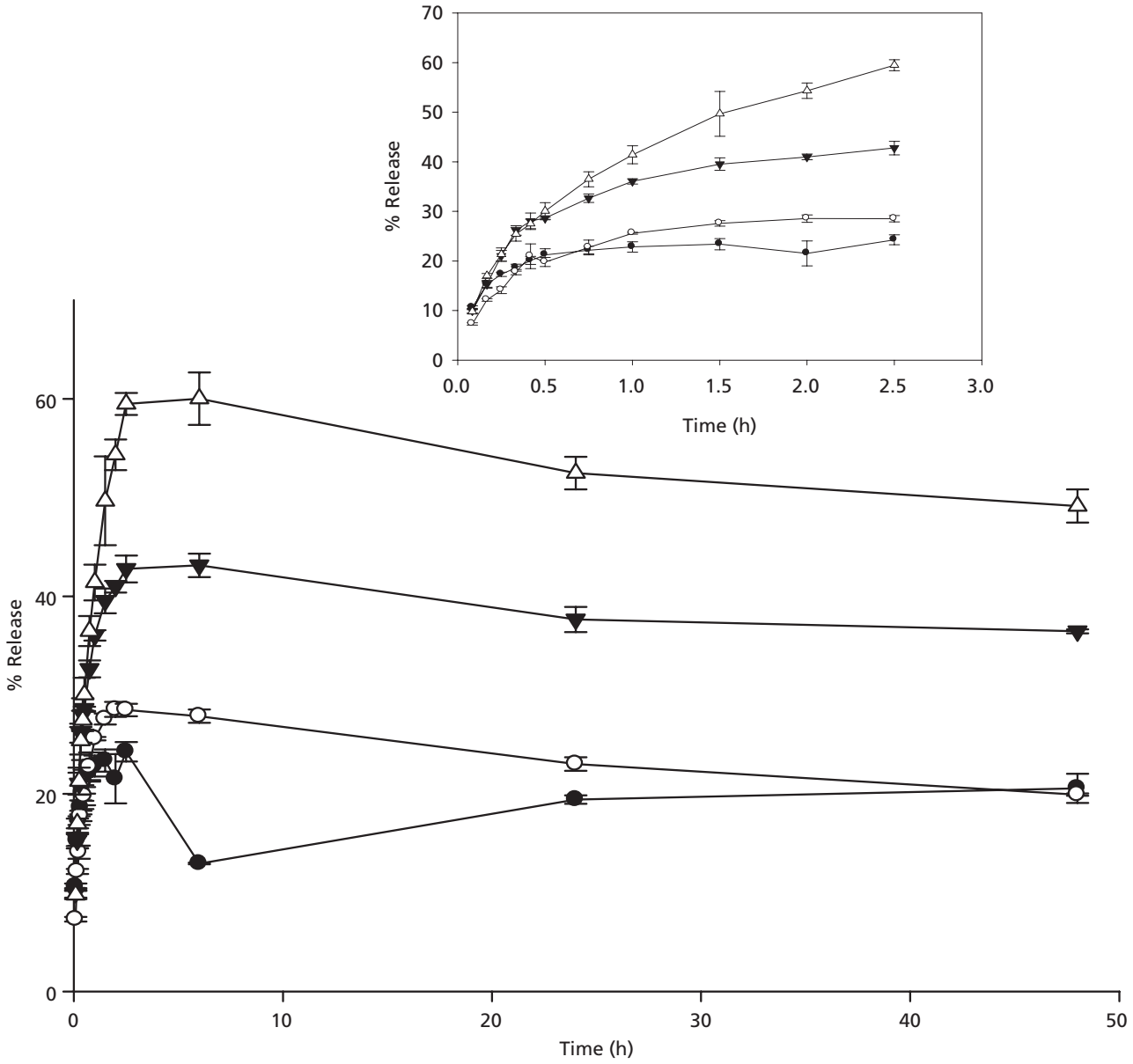

Figure 1 Dissolution profile of Tegretol® tablets in the absence (●) and presence of 0.5 (o), 2 (▼) and 4 (*Δ*) mM of TPGS at 10°C. The insert shows the first 2.5 h.

temperature (25°C; Figure 2). In this work, dissolution studies were carried out with a commercially available formulation of CBZ (Tegretol®), in a medium with various concentrations of surfactant (TPGS), and a shorter transformation stage was expected. In fact, this shorter transformation stage *was* observed and is clearly depicted in the dissolution profile at 6 h (25°C; Figure 2).

More specifically, at 25°C, all four dissolution profiles exhibited the same pattern up to 6 h, i.e. CBZ concentrations increase up to 2.5 h and then decrease rapidly between 2.5 and 6 h (Figure 2). After this time point CBZ concentrations remain constant in the presence of 0, 0.5 mM TPGS, while CBZ concentrations increase again in the presence of 2 and 4 mM of TPGS. CBZ's dissolution maximum concentration in the presence of 4 mM TPGS was 70% higher than the dissolution maximum concentration in the absence of the surfactant and 157% higher than CBZ's aqueous solubility at 25°C (104.9 ± 6.21 μg/ml; Figure 4). These increases are 50% less than the ones observed at 10°C. These results indicate that TPGS at 25°C affects the dissolution kinetics of CBZ in a less concentration-dependent manner than at 10°C (Figures 1, 2 and 4). In all these cases, statistical comparisons resulted in statistically significant differences.

In the dissolution studies performed in the presence of TPGS at 10°C, the dissolution pattern that was observed was similar to the one at 25°C. A steady-state value was reached at 48 h following a smooth concentration diminution after the peak concentration, which was observed between 2.5–6 h (Figure 1) but no re-increase of the concentration was observed. On the contrary, in the absence of TPGS at 10°C,

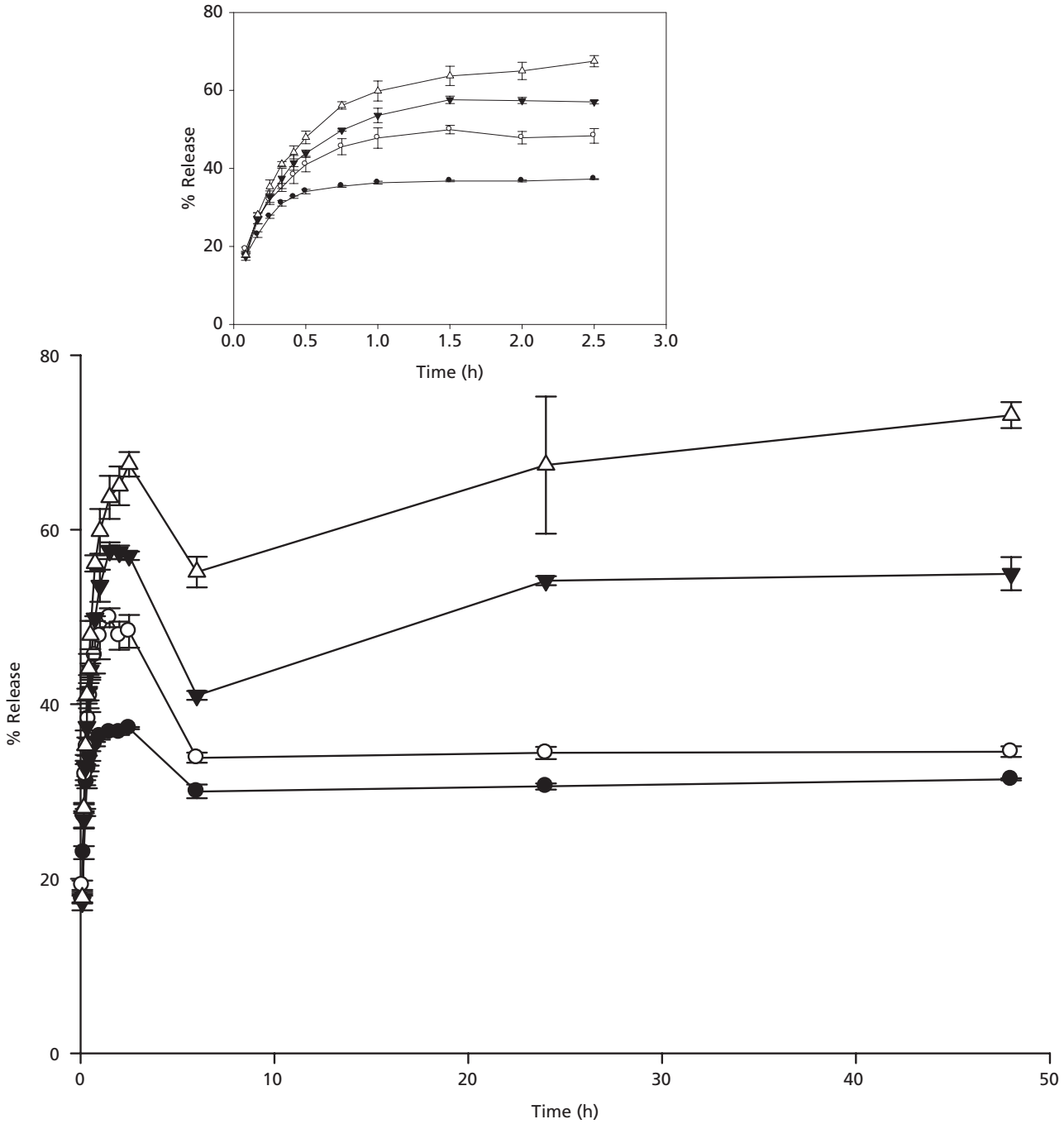

Figure 2 Dissolution profile of Tegretol® tablets in the absence (●) and presence of 0.5 (o), 2 (▼) and 4 (Δ) mM of TPGS at 25°C. The insert shows the first 2.5 h.

CBZ concentration declined between 2.5 and 6 h, followed by a gradual increase (Figure 1). These results clearly demonstrate that TPGS at 10°C dramatically affects the dissolution kinetics of CBZ, and in a concentration-dependent manner (Figures 1 and 4). In fact, the maximum CBZ concentration observed in the dissolution studies in the presence of 4 mM TPGS, increased by up to 147% compared to the dissolution concentration maximum in the absence of the surfactant, and up to 292% compared to CBZ's aqueous solubility at 10°C (Figure 4). In other words, TPGS facilitates the initial dissolution rate of CBZ by reducing the energy barrier for the interfacial transport of CBZ molecules from the solid to the aqueous phase, resulting in high concentration dissolution maxima. This effect seems to be more intense and patent at 10°C. It is well known that hydrophobic interactions become predominant in binding phenomena at low temperatures.[41] This type of interactions seem to operate at the solid–liquid interface at 10°C. These observations are also in accord with the minor effect of excipients on CBZ solubility at 10°C. Thus, CBZ's solubility is increased only 8.8% (66.48 ± 2.22 μg/ml)

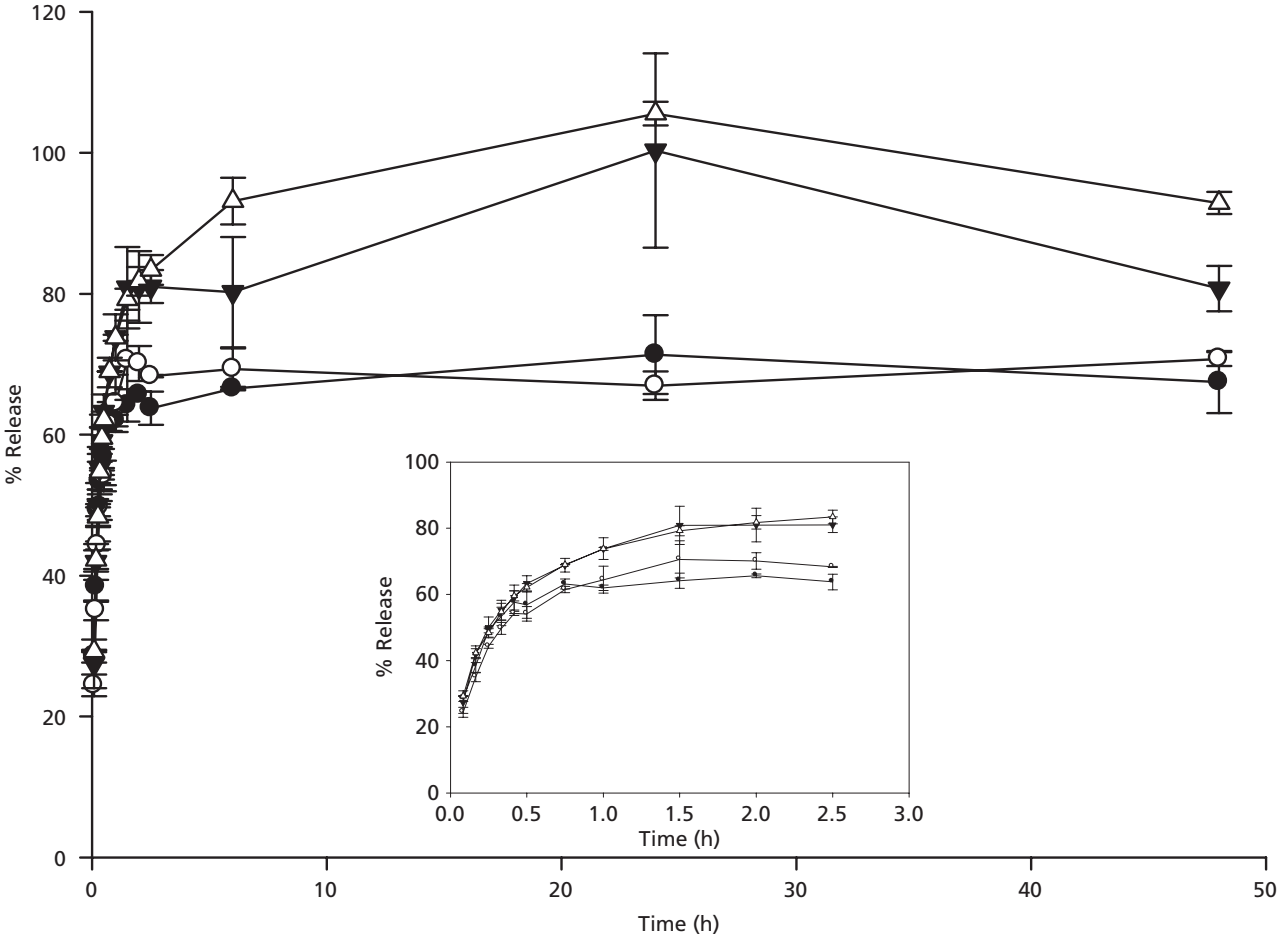

Figure 3 Dissolution profile of Tegretol® tablets in the absence (●) and presence of 0.5 (o), 2 (▼) and 4 (Δ) mM of TPGS at 37°C. The insert shows the first 2.5 h.

Table 1 Carbamazepine's saturation solubility (C_s) and maximum concentration (C_{max}) observed in dissolution experiments in the presence and absence of TPGS at 10, 25 and 37°C

TPGSmM	10°C		25°C		37°C	
	$C_s \pm$ SD (μg/ml)	$C_{max} \pm$ SD (μg/ml)	$C_s \pm$ SD (μg/ml)	$C_{max} \pm$ SD (μg/ml)	$C_s \pm$ SD (μg/ml)	$C_{max} \pm$ SD (μg/ml)
0	61.1 ± 1.5	97.1 ± 1.0	104.9 ± 6.21	149.02 ± 0.13	186.18 ± 10.61	268.94 ± 2.01
0.5	64.63 ± 8.65	114.19 ± 0.75	111.81 ± 7.35	199.65 ± 1.1	202.09 ± 1.3	283.69 ± 3.7
2	67.23 ± 6.63	171.11 ± 1.35	165.8 ± 9.25	230.38 ± 0.95	274.24 ± 5.81	378 ± 4.7
4	89.9 ± 8.33	240.08 ± 2.66	158.55 ± 2.97	269.99 ± 1.4	312.29 ± 11.05	398.96 ± 1.5

in the presence of 40 mg microcrystalline cellulose and 19.1% (72.8 ± 2.1 μg/ml) in the presence of 0.70 mg of silicon dioxide, respectively, compared to CBZ's aqueous solubility (61.1 ± 1.5 μg/ml; Table 2).

These results indicate that the effect of TPGS on the interfacial transport of CBZ molecules from the solid to the aqueous phase, observed at 10°C, seems also to operate at 25°C. However, its contribution towards the increase of the CBZ dissolution rate and the dissolution maximum is less important at 25°C, if one takes into account that the effect of excipients (Table 2) as well as 2 and 4 mM TPGS (Table 1 and Figure 4) on CBZ solubility cannot be ignored.

The dissolution results obtained at 37°C (Figure 3) are dissimilar to the data recorded at 10°C and 25°C (Figures 1 and 2). Thus, the transition between the polymorphs can be hardly seen between 3 and 6 h for the dissolution data carried out in 0.5 and 2 mM TPGS. The effect of TPGS on the CBZ dissolution rate is not any more concentration-dependent, and mirrors the effect of TPGS on CBZ solubility. This observation can be explained on the basis of the parallel lying of data points relative to the concordance line of Figure 4. Besides this, there is an appreciable effect of the excipients on CBZ solubility (Table 2).

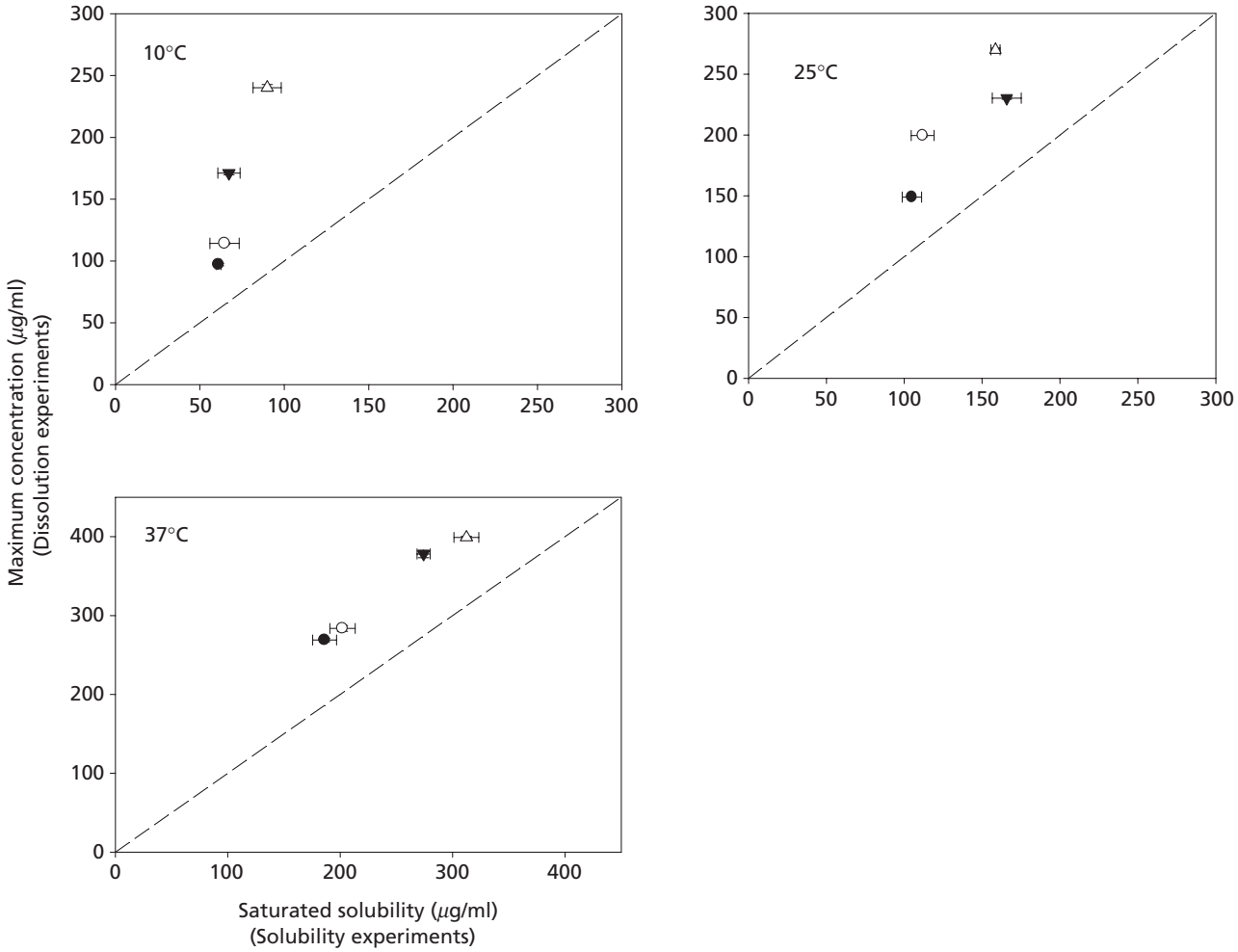

Figure 4 Maximum CBZ concentrations observed in dissolution experiments as a function of saturation solubility. The dashed line is the concordance line. H_2O (●), 0.5 mM TPGS (○), 2 mM TPGS (▼) and 4 mM TPGS (Δ). Data shown as mean ± SD in all graphs.

Table 2 Carbamazepine's saturation solubility (C_s) in the presence of microcrystalline cellulose or silicon dioxide at 10, 25 and 37°C

Excipient	C_s ± SD (10°C) (μg/ml)	C_s ± SD (25°C) (μg/ml)	C_s ± SD (37°C) (μg/ml)
Microcrystalline cellulose (mg)			
40	66.48 ± 2.22	149.62 ± 1.68	246.9 ± 0.71
70	63.93 ± 2.43	135.48 ± 3.72	237.14 ± 3.28
Silicon dioxide (mg)			
0.35	69.9 ± 0.9	143.25 ± 8.73	248.21 ± 6.46
0.70	72.8 ± 2.1	135.22 ± 3.21	243.84 ± 3.67

The various processes involved in the dissolution of CBZ tablets in the presence of TPGS are multiple and complex. Figure 5 illustrates a proposed model describing the equilibria of CBZ in aqueous solution containing a surfactant (TPGS). Initially, the CBZ tablet disintegrates and the drug and the SiO_2 and microcrystalline cellulose particles are released. The dissolution of drug particles to CBZ dissolved species (anhydrous polymorph) is followed by: (i) transition to dihydrated form, (ii) adsorption to undissolved species and (iii) micellization. These processes occur simultaneously while some of them are reversible (Figure 5). In fact, the initial anhydrous form of CBZ is transformed to the dihydrate form (more stable), but as this conversion is incomplete,[40] in the final solution both forms (anhydrous and dihydrated) co-exist. It should be noted that the critical micelle concentration of TPGS is 0.132 mM at 37°C,[42] which is below the concentration range used in this study. The relative importance of kinetics/dynamics for each one of the phenomena depicted in Figure 5 is not only dependent on TPGS concentration used, but also on the temperature of the experiments. At 10°C, in the

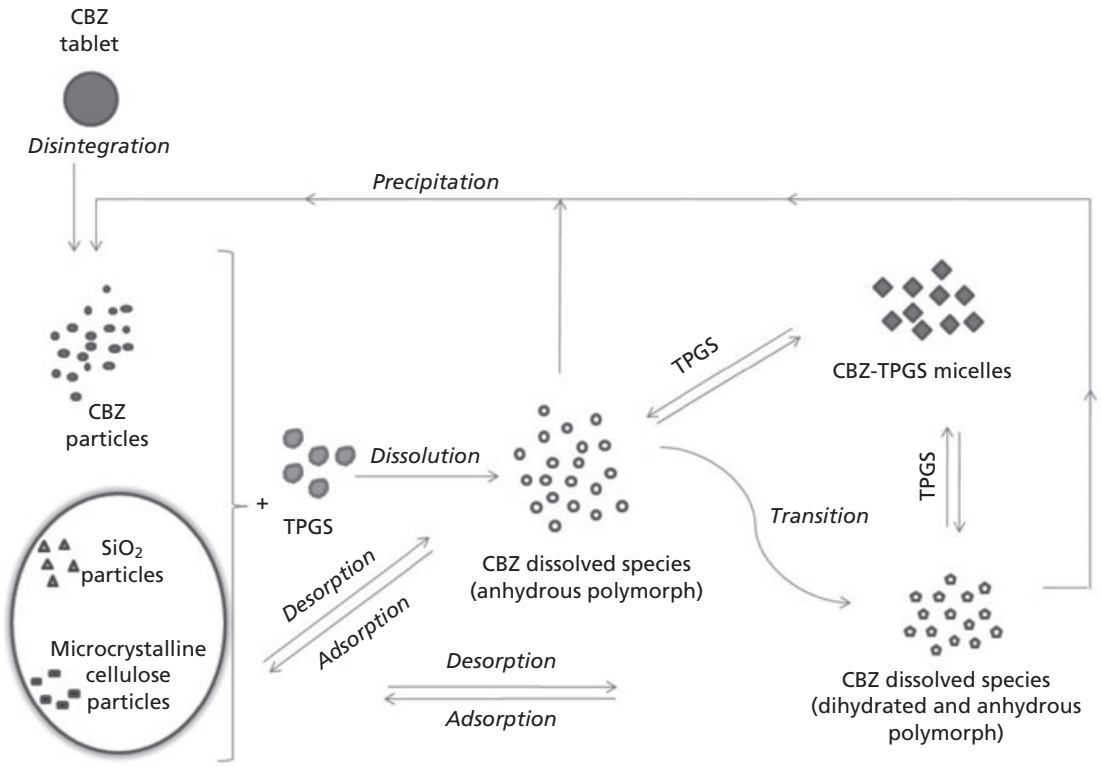

Figure 5 The various processes involved in the dissolution of CBZ tablets in the presence of TPGS.

absence of TPGS, transformation between the polymorphs seems to be terminated at 6 h. Then, an increase of CBZ concentration follows (Figure 1), resulting from changes in the equilibria of adsorption–desorption of CBZ in the solid particles of the excipients (Figure 5). The dissolution data at 10°C in the presence of 0.5, 2 and 4 mM TPGS follow the classical pattern of supersaturated dissolution curves (Figure 1). Since the effect of TPGS on dissolution concentration maxima is concentration-dependent (Figure 4) the kinetics of CBZ dissolution can be explained with a reaction-limited model (Equation 2), with the TPGS molecules playing the role of reaction species, as explained in the previous section. Thus, the rate of the dissolution process for the reaction-limited model of dissolution based on Equation 2 is given by the velocity of the unidirectional reaction:[29]

$$\frac{dC}{dt} = k_1^*\left(\frac{M_0}{V} - C\right)^a - k_{-1}C \qquad (4)$$

where C is the concentration of the dissolved drug, $k_1^* = k_1[w_0]^b$, M_0 is the initial quantity (dose) in mass units, a and b are constants related to stoichiometry of the reaction and also to the geometry of the particles and $[w_0]$ is the concentration of the free TPGS at $t = 0$.

Although in the original work,[29] k_1^* was assumed to be constant, a time-dependent expression of the following form may also be appropriate:

$$k_1^* = K \cdot t^{-h} \qquad (5)$$

where K is a constant in $(\text{time})^{h-1}$ units. Expressions of this form have been used previously to account for time-variable rate coefficients, due to understirring and crowding in the microenvironment of the reaction.[43,44] This approach is often referred to as fractal kinetics[43] and has implications and physical meaning beyond an empirical time-dependent coefficient. For the purposes of the this study, Equation 5 can be also considered appropriate, not only for the topological constraints in the solid–liquid interface, but also for the solubility changes during dissolution due to time-dependent transitions in pharmaceutical polymorphs. In order to avoid infinity at time zero, an expression similar to Equation 5 is considered:

$$k_1^* = K(\lambda + (1+t)^{-h}) \qquad (6)$$

where λ is a constant, in $(\text{time})^{-h}$ units, preventing the entire expression from approaching zero for large times. As far as precipitation is concerned (Figure 5), this has been described as a first-order process governed by the first-order rate constant k_{-1} (Equation 4).

Equations 4 to 6 describe a dissolution process in which the solubility, as given by Equation 3, is initially higher and drops with time. Equations 4–6 were fitted to the experimental data of CBZ in the presence of 0.5, 2 and 4 mM TPGS at 10°C. Due to the high correlation of parameters K and a, which made the fit of Equations 4–6 to experimental data unstable, parameter a was fixed to 1 to improve the stability and convergence of the regression analysis. Parameter estimates are

Table 3 Parameter estimates of three datasets of Tegretol® tablets at 10°C exhibiting supersaturated dissolution profiles

TPGS (mM)	K (min^{h-1} mg/l)	CV	k_1 (min^{-1})	CV	λ (min^{-h})	CV	h	CV
0.5	0.0284	0.17	0.00873	0.26	0.0730	0.42	0.603	0.12
2	0.0448	0.13	0.00540	0.25	0.0643	0.38	0.665	0.07
4	0.0299	0.098	0.00292	0.17	0.0501	0.37	0.396	0.10

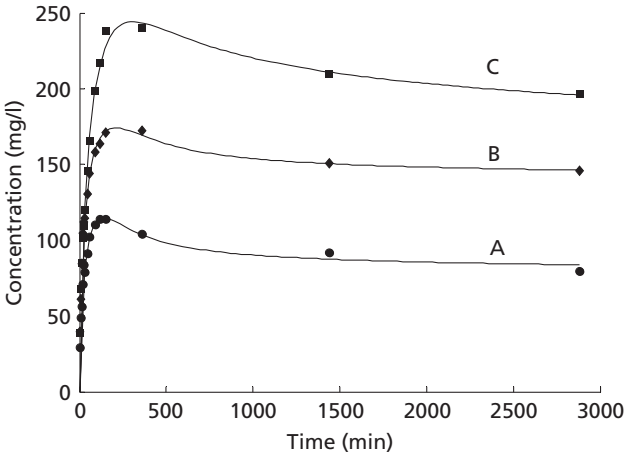

Figure 6 Fits of Equations 4 and 6 to three datasets of Tegretol® tablets at 10°C, exhibiting supersaturated dissolution profiles. A, 0.5 mM TPGS; B, 2 mM TPGS; C, 4 mM TPGS.

tabulated, together with the respective coefficients of variation (CV) values, in Table 3. In Figure 6 the profiles of the fitted model are plotted together with the data points, demonstrating visually that the model adequately describes the data. Although the fundamental parameter k_1^* of the model is time-dependent (Equation 5), an estimate can be derived from Equation 4 at t_{max} using $a = 1$ and $dC/dt = 0$:

$$0 = k^*_{1t\,\max}\left(\frac{M_0}{V} - C_{\max}\right) - k_{-1}C_{\max} \quad (7)$$

which leads to:

$$(k_1^*)_{t\,\max} = k_{-1}C_{\max} / \left(\frac{M_0}{V} - C_{\max}\right) \quad (8)$$

Using the estimates for k_{-1} listed in Table 3 and the C_{max} values listed in Table 1, the estimates 3.5, 2.2 and 1.2 10^{-3}/min for $(k_1{*})_{tmax}$ were derived from Equation 8 for 0.5, 2.0 and 4.0 mM TPGS, respectively. This indicates that estimates for the principal parameter controlling the reaction-limited model of drug dissolution, k_1^*, cannot only be obtained from typical dissolution data of a monotonic nature,[29] but also from classical supersaturated dissolution curves. This finding allows one not only to quantify and rank dissolution data of marketed drugs for biopharmaceutical classification purposes but also to utilize dissolution specifications of the compendia for comparative purposes. Work in this direction is now in progress in our laboratory.

Conclusions

Overall, vitamin E TPGS increased the solubility and dissolution rate of CBZ at all temperatures studied. The pattern of the dissolution curves varies with temperature and mirrors the dynamics of the various processes and equilibria involved (Figure 5). The modification of the reaction-limited model of dissolution[29] allowed us to describe classical supersaturated dissolution curves mathematically. Since the mechanism of drug dissolution in the gastrointestinal tract may exhibit departures from a classic diffusion-limited dissolution process,[45] the proposed reaction-limited model may have certain advantages. This is particularly so if one takes into account that recent reports in the literature[14] indicate that *in vivo* dissolution conditions favour supersaturated drug solutions.

Declarations

Acknowledgements

The authors wish to thank Dr A. Iliadis, University of Marseilles, for his advice on the modelling aspects of the study.

Conflict of interest

The Author(s) declare(s) that they have no conflicts of interest to disclose.

Funding

This research has received no specific grant from any funding agency in the public, commercial or not-for-profit sectors.

References

1. Zhou H *et al*. Hydrophobic ion pairing of isoniazid using a prodrug approach. *J Pharm* 2002; 91: 1502–1511.
2. Vogt M *et al*. Dissolution improvement of four poorly water soluble drugs by cogrinding with commonly used excipients. *Eur J Pharm Biopharm* 2008; 68: 330–337.
3. Janssens S *et al*. Formulation and characterization of ternary solid dispersions made up of Itraconazole and two excipients, TPGS 1000 and PVPVA 64, that were selected based on a supersaturation screening study. *Eur J Pharm Biopharm* 2008; 69: 158–166.
4. Konno H *et al*. Effect of polymer type on the dissolution profile of amorphous solid dispersions containing felodipine. *Eur J Pharm Biopharm* 2008; 70: 493–499.
5. Shiraki K *et al*. Dissolution improvement and the mechanism of the improvement from cocrystallization of poorly water-soluble compounds. *Pharm Res* 2008; 25: 2581–2592.
6. Dhumal RS *et al*. Cefuroxime axetil solid dispersion with polyglycolized glycerides for improved stability and bioavailability. *J Pharm Pharmacol* 2009; 61: 743–751.

7. Sethia S, Squillante E. Physicochemical characterization of solid dispersions of carbamazepine formulated by supercritical carbon dioxide and conventional solvent evaporation methods. *J Pharm Sci* 2002; 91: 1948–1957.
8. Sethia S, Squillante E. Solid dispersion of carbamazepine in PVP K30 by conventional solvent evaporation and supercritical methods. *Int J Pharm* 2004; 272: 1–10.
9. Iervolino M *et al*. Membrane penetration enhancement of ibuprofen using supersaturation. *Int J Pharm* 2000; 198: 229–238.
10. Larrucea E *et al*. Study of the complexation behavior of tenoxicam with cyclodextrins in solution: improved solubility and percutaneous permeability. *Drug Dev Ind Pharm* 2002; 28: 245–252.
11. Gohel MC, Patel LD. Processing of nimesulide-PEG 400-PG-PVP solid dispersions: preparation, characterization, and in vitro dissolution. *Drug Dev Ind Pharm* 2003; 29: 299–310.
12. Park SH, Choi HK. The effects of surfactants on the dissolution profiles of poorly water-soluble acidic drugs. *Int J Pharm* 2006; 321: 35–41.
13. Kalantzi L *et al*. Canine intestinal contents vs. simulated media for the assessment of solubility of two weak bases in the human small intestinal contents. *Pharm Res* 2006; 23: 1373–1381.
14. Brouwers J *et al*. In vitro behavior of a phosphate ester prodrug of amprenavir in human intestinal fluids and in the Caco-2 system: illustration of intraluminal supersaturation. *Int J Pharm* 2007; 336: 302–309.
15. Brouwers J *et al*. Parallel monitoring of plasma and intraluminal drug concentrations in man after oral administration of fosamprenavir in the fasted and fed state. *Pharm Res* 2007; 24: 1862–1869.
16. Clarysse S *et al*. Postprandial changes in solubilizing capacity of human intestinal fluids for BCS class II drugs. *Pharm Res* 2009; 26: 1456–1466.
17. Leuner C, Dressman J. Improving drug solubility for oral delivery using solid dispersions. *Eur J Pharm Biopharm* 2000; 50: 47–60.
18. Hancock B, Parks M. What is the true solubility advantage for amorphous pharmaceuticals? *Pharm Res* 2001; 17: 397–404.
19. Rogers TL *et al*. Development and characterization of a scalable controlled precipitation process to enhance the dissolution of poorly water-soluble drugs. *Pharm Res* 2004; 21: 2048–2057.
20. Raghavan SL *et al*. Effect of cellulose polymers on supersaturation and in vitro membrane transport of hydrocortisone acetate. *Int J Pharm* 2000; 193: 231–237.
21. Raghavan SL *et al*. Membrane transport of hydrocortisone acetate from supersaturated solutions; the role of polymers. *Int J Pharm* 2001; 221: 95–105.
22. Gunawan LG *et al*. Structural relaxation of acetaminophen glass. *Pharm Res* 2006; 23: 967–979.
23. Yamamoto K *et al*. Dissolution behavior and bioavailability of phenytoin from a ground mixture with microcrystalline cellulose. *J Pharm Sci* 1976; 65: 1484–1488.
24. Fujii M *et al*. Dissolution and bioavailability of phenobarbital in solid dispersion with phosphatidylcholine. *Chem Pharm Bull* 1991; 39: 1886–1888.
25. Suzki H, Sunada H. Influence of water-soluble polymers on the dissolution of nifedipine solid dispersions with combined carriers. *Chem Pharm Bull* 1998; 46: 482–487.
26. Urbanetz NA. Stabilization of solid dispersions of nimodipine and polyethylene glycol 2000. *Eur J Pharm Sci* 2006; 28: 67–76.
27. Valsami G *et al*. Modeling of supersaturated dissolution data. *Int J Pharm* 1999; 181: 153–157.
28. Kaneniwa N *et al*. Dissolution behaviour of carbamazepine polymorphs. *Yakugaku Zasshi* 1987; 107: 808–813.
29. Dokoumetzidis A *et al*. Development of a reaction-limited model of dissolution: Application to official dissolution tests experiments. *Int J Pharm* 2008; 355: 114–125.
30. Sugano K. A simulation of oral absorption using classical nucleation theory. *Int J Pharm* 2009; 378: 142–145.
31. Sugano K. Computational oral absorption simulation for low-solubility compounds. *Chem Biodivers* 2009; 6: 2014–2029.
32. Kobayashi Y *et al*. Physicochemical properties and bioavailability of carbamazepine polymorphs and dihydrate. *Int J Pharm* 2000; 193: 137–146.
33. Tian F *et al*. Influence of polymorphic form, morphology, and excipient interactions on the dissolution of carbamazepine compacts. *J Pharm Sci* 2007; 96: 584–594.
34. Sokol RJ *et al*. Improvement of cyclosporin absorption in children after liver transplantation by means of water-soluble vitamin E. *Lancet* 1991; 338: 212–214.
35. Ismailos G. *In Vitro and in Vivo Studies on Cyclosporin Absorption Characteristics*. Athens, Greece: National and Kapodistrian University of Athens, 1999. (dissertation).
36. Dokoumetzidis A, Macheras P. A century of dissolution research: From Noyes and Whitney to the Biopharmaceutics Classification System. *Int J Pharm* 2006; 321: 1–11.
37. Dejmek M, Ward CA. A statistical rate theory study of interface concentration during crystal growth or dissolution. *J Chem Phys* 1998; 108: 8698–8704.
38. Getsoian A *et al*. One-solvent polymorph screen of carbamazepine. *Int J Pharm* 2008; 348: 3–9.
39. Urakami K *et al*. A novel method for estimation of transition temperature for polymorphic pairs in pharmaceuticals using heat of solution and solubility data. *Chem Pharm Bull (Tokyo)* 2002; 50: 263–267.
40. Lehto P *et al*. Solvent-mediated solid phase transformations of carbamazepine: effects of simulated intestinal fluid and fasted state simulated intestinal fluid. *J Pharm Sci* 2009; 98: 985–996.
41. Sideris EE *et al*. Determination of association constants in cyclodextrin/drug complexation using the Scatchard plot: application to beta-cyclodextrin-anilinonaphthalenesulfonates. *Pharm Res* 1992; 9: 1568–1574.
42. Zografi G *et al*. Disperse systems. Surfactant properties in solutions and micelle formulation. *Remington's Pharmaceutical Sciences*, 18th edn. Easton, Pennsylvania: Mack Publishing Company, 18042, 1990: 257–309.
43. Kopelman R. Fractal reaction-kinetics. *Science* 1988; 241: 1620–1626.
44. Macheras P, Dokoumetzidis A. On the heterogeneity of drug dissolution and release. *Pharm Res* 2000; 17: 108–112.
45. Persson EM *et al*. The effects of food on the dissolution of poorly soluble drugs in human and in model small intestinal fluids. *Pharm Res* 2005; 22: 2141–2151.